Infrared Spectra of Magnesium Hydride Molecules, Complexes, and Solid Magnesium Dihydride

Xuefeng Wang and Lester Andrews*

Department of Chemistry, University of Virginia, Charlottesville, Virginia 22904-4319

Received: August 10, 2004; In Final Form: September 29, 2004

Laser-ablated Mg atoms react with molecular hydrogen to give magnesium hydrides during condensation in excess hydrogen and neon for characterization by matrix infrared spectroscopy. The observed absorptions are identified by isotopic substitution and theoretical calculations of vibrational fundamentals and assigned to the MgH, MgH_2, Mg_2H, Mg_2H_2, Mg_2H_3, and Mg_2H_4 molecules. Subsequent UV irradiation excites Mg to the ^1P state, which inserts into H_2 and markedly increases the yield of MgH_2 and Mg_2H_4. Interesting $MgH_2(H_2)_n$ complexes are formed with high yield in solid hydrogen. Mg_2H_4 is a dibridged molecule analogous to dialane. Sample annealing gives MgH_2 polymers, which favor single bridge-bond linkages. Warming above 8 K allows the H_2 matrix to evaporate and solid MgH_2 to form with broad 1160 and 560 cm^{-1} absorptions that remain on the window at 300 K. Thus, we have reacted the elements to give the stable MgH_2 molecule, formed its dimer and tetramer, and finally obtained the ultimate polymer, solid MgH_2, which is of interest for hydrogen storage.

Introduction

Magnesium hydrides continue to be of interest as promising materials for hydrogen storage.[1–3] MgH_2 is a stable molecule with a high hydrogen storage capacity (7.6 wt %). However, reversibility of the thermal absorption/desorption is very poor, and a temperature near 300 °C is required for 1 bar of hydrogen gas. Experiments show that magnesium hydride formation from bulk Mg and H_2 gas is very slow, but Mg alloys with transition metals react with molecular hydrogen to form hydrides fairly rapidly where transition metals act as a catalyst to decompose molecular hydrogen. Magnesium hydride solid forms the rutile structure, and vibrational spectra have been recorded by inelastic-neutron and Raman scattering.[4,5] The gaseous linear MgH_2 molecule has recently been observed in an electrical discharge through the vibration–rotation emission spectrum.[6]

The reaction of laser-ablated Mg atom with H_2 in excess argon has been studied in this group, and the magnesium hydride molecules MgH, Mg_2H_2, MgH_2, and Mg_2H_4 have been identified.[7] Magnesium dihydride has also been observed in solid krypton and xenon.[8] Recently we reported the preparation of dialane (Al_2H_6) using the reaction of laser-ablated aluminum with pure H_2 during codensation at 3.5 K.[9–11] The AlH generated from laser ablation further reacts with H_2 to give AlH_3 upon UV photolysis, which dimerizes to form Al_2H_6.[9,10] Evidence for trialane (Al_3H_9) and tetraalane (Al_4H_{12}) as stable molecules was found in our later investigation.[11] Similarly gallium, indium, and thallium hydride molecules have been prepared and investigated in solid hydrogen, and solid Ga and In hydrides were formed on evaporation of the hydrogen matrix.[12–15]

We present here a new matrix isolation study of laser-ablated magnesium atom reactions with H_2 in solid hydrogen and neon. The higher magnesium hydrides Mg_2H_2, Mg_2H_3, Mg_2H_4, Mg_3H_6, and Mg_4H_8 and hydrogen complexes $MgH_2(H_2)_n$ are

identified by matrix infrared spectroscopy and density functional theoretical calculations. The characterization of higher magnesium hydrides and dihydrogen complexes can provide important molecular structure information for approaching more efficient Mg-based hydrogen-storage materials.

Experimental and Computational Methods

The experiments for reactions of laser-ablated magnesium atoms with hydrogen during condensation in excess hydrogen and neon have been described in detail previously.[16–18] The Nd: YAG laser fundamental (1064 nm, 10 Hz repetition rate with 10 ns pulse width) was focused onto a rotating normal magnesium target (Fisher) or ^{26}Mg plate (Oak Ridge National Laboratory). The laser energy was varied from 5 to 20 mJ/pulse. Laser ablated magnesium atoms were co-deposited with hydrogen (0.2 to 4%) in excess neon or pure hydrogen onto a 3.8 K CsI cryogenic window at 2–4 mmol/h (H_2/Ne for 1 h and pure H_2 for 30 min). Isotopic D_2 and HD (Cambridge Isotopic Laboratories) and selected mixtures were used in different experiments. FTIR spectra were recorded at 0.5 and 0.13 cm^{-1} resolution on a Nicolet 750 with 0.1 cm^{-1} accuracy, using an HgCdTe detector. Matrix samples were annealed at different temperatures, and selected samples were subjected to broadband photolysis by a medium-pressure mercury arc lamp (Philips, 175W) with the globe removed or ArF eximer (193 nm) irradiation (Optex). A simple and efficient converter was used to prepare parahydrogen and several spectra of Mg atom reaction with p-H_2 were collected.[19] Emission spectra were recorded with an Ocean Optics optical fiber spectrometer.[20]

The density functional theoretical calculations of magnesium hydrides and hydride hydrogen complexes are given for comparison. The Gaussian 98 program[21] was employed to calculate the structures and frequencies of expected molecules, using the B3LYP functional and the MP2 method. The 6-311++G(3df,3pd) basis set for both Mg and H atoms was used. All the geometrical parameters were fully optimized and

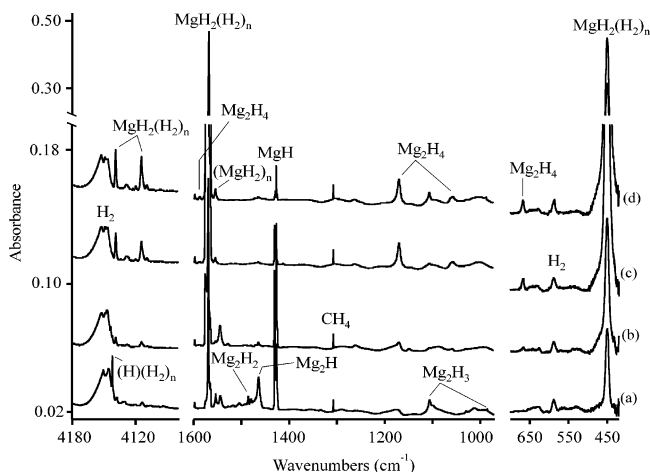* Address correspondence to this author. E-mail: lsa@virginia.edu.

Figure 1. Infrared spectra in selected regions for laser-ablated Mg co-deposited with n-H$_2$ at 3.8 K: (a) after deposition for 20 min, (b) after $\lambda > 320$ nm irradiation for 20 min, (c) after 240−380 nm irradiation for 20 min, and (d) after annealing to 6.6 K.

the harmonic vibrational frequencies were obtained analytically at the optimized structures.

Results

Experimental spectra are presented for magnesium atom reactions with H$_2$, D$_2$, HD, and the H$_2$ + D$_2$ mixture in excess neon and solid molecular hydrogen. Similar experiments have been done in parahydrogen and orthodeuterium for comparison.[22,23] Common absorptions, namely those assigned to H(H$_2$)$_n$ and H$^-$(H$_2$)$_n$, have been reported previously,[18,24] and are not discussed here. Trace impurity CO$_2$, CO, H$_2$O, and CH$_4$ appeared in all experiments but no impurity reaction products were observed with these molecules. New DFT and MP2 calculations of magnesium hydrides and hydrogen complexes are given for identification purposes.

Infrared Spectra. Figure 1 shows the spectra of laser-ablated magnesium atom with pure normal H$_2$ during co-deposition at
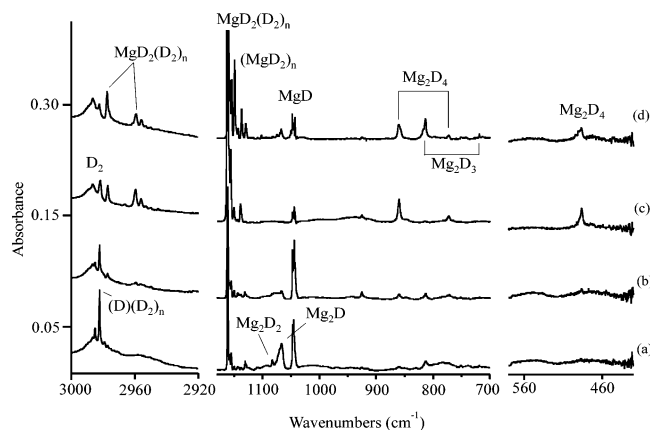

Figure 2. Infrared spectra in selected regions for laser-ablated Mg co-deposited with n-D$_2$ at 3.8 K: (a) after deposition for 20 min, (b) after $\lambda > 320$ nm irradiation for 20 min, (c) after $\lambda > 240$ nm irradiation for 20 min, and (d) after annealing to 10.5 K.

3.8 K, and the absorptions are listed in Table 1. After deposition new bands at 4139.0, 4114.5, 1569.5 (site splitting at 1576.4 cm^{-1}), and 450.1 cm^{-1} (group A), weak bands at 1587.6, 1170.5, 1058.7, and 667.2 cm^{-1} (group B), a strong 1427.1 cm^{-1} band (site splittings at 1429.5, 1430.6, and 1431.9 cm^{-1}), and weak absorptions at 1464.6 and 1105.9 cm^{-1} were observed. Irradiation at $\lambda > 320$ nm increased the group A and B bands, markedly reduced the 1464.6 and 1105.9 cm^{-1} absorptions, and decreased the 1544.3 cm^{-1} satellite. Subsequent 240−380 nm irradiation increased group A and B bands by a factor of 6, and the following $\lambda > 240$ nm irradiation increased group A and decreased group B. Annealing to 6.6 K then decreased the group A and increased the group B bands (Figure 1d). A subsequent annealing to 8.0 K (not shown) decreased the group A and B bands, sharpened the major band at 1569.2 cm^{-1}, revealed magnesium isotopic splittings at 1566.9 and 1565.2 cm^{-1}, and further increased a 1554.5 cm^{-1} satellite absorption. In solid normal deuterium group A bands shift to 2977.2, 2959.5, and 1161.4 cm^{-1} (the 450.1 cm^{-1} band shifts out of our measure-

TABLE 1: Infrared Absorptions (cm^{-1}) Observed from Reactions of Magnesium and Dihydrogen in Excess Hydrogen

Mg n-H$_2$	Mg p-H$_2$	^{26}Mg n-H$_2$	Mg n-D$_2$	Mg o-D$_2$	^{26}Mg n-D$_2$	HD	identification
4139.0	4148.8	4139.0	2977.2	2986.7	2977.2	3620.0	MgH$_2$(H$_2$)$_n$
4114.5	4128.0	4114.5	2959.5	2959.8	2959.5	3597.6	MgH$_2$(H$_2$)$_n$
3078.8	3091.6	3073.0	2249.4	2252.3	2242.7		MgH$_2$(H$_2$)$_n$ (overtone)
						1594.0, 1592.6	Mg$_2$H$_2$D$_2$
1587.6		1583.7					Mg$_2$H$_4$
1576.4			1163.2				MgH$_2$(H$_2$)$_n$ (site)
1569.5	1577.4[a]	1565.2	1161.4	1163.7	1155.9	1575.6, 1166.0	MgH$_2$(H$_2$)$_n$
1554.5			1150.7			1554.4, 1130.3	(MgH$_2$)$_n$
1544.3	1546.6		1138.3	1140.6			(Mg$_x$H)
						1567.2, 1139.1	MgHD(HD)$_n$
1486.1	1491.6	1484.1	1083.0	1084.7	1080.8	1495.7, 1088.9	Mg$_2$H$_2$
1480.4		1478.5				1489.1, 1084.5	Mg$_2$H$_2$ (site)
1464.6	1466.7	1462.6	1066.6	1068.7	1063.8	1464.3, 1067.8	Mg$_2$H
1431.9		1429.8	1047.5	1048.0	1045.0	1433.5, 1046.9	MgH (site)
1430.6		1428.5	1045.9	1046.4	1043.4	1431.9, 1045.5	MgH (site)
1429.5	1429.9	1427.4	1044.4	1044.9	1041.8	1430.6, 1044.3	MgH (site)
1427.1	1427.4	1425.3	1042.8	1043.0	1039.9	1428.1, 1042.6	MgH
1170.5	1168.2	1169.0	859.9	859.8	857.9	1169, 1146.3	Mg$_2$H$_4$
						811.0, 807.9	HMg(HD)MgD
						860.8, 771.1	HMg(D$_2$)MgH
						1204.9, 655.5	DMg(H$_2$)MgD
1105.9	1106.8	1105.6	813.1	813.4	811.6	1013.9, 834.3	Mg$_2$H$_3$
1058.7	1057.1	1057.0	772.3	772.4	770.8		Mg$_2$H$_4$
985.5	986.1	985.1	718.5	718.6	717.7		Mg$_2$H$_3$
667.2	665.3	666.1	486.5	486.1	485.0	586.3, 505.3	Mg$_2$H$_4$
450.1	450.4	449.0					MgH$_2$(H$_2$)$_n$

^{a} For ^{24}Mg: ^{25}Mg at 1575.1 cm^{-1}, ^{26}Mg at 1573.0 cm^{-1}. ^{b} For ^{24}Mg: ^{25}Mg at 1160.7 cm^{-1}, ^{26}Mg at 1157.7 cm^{-1}.

Magnesium Hydrides, Complexes, and Dihydrides

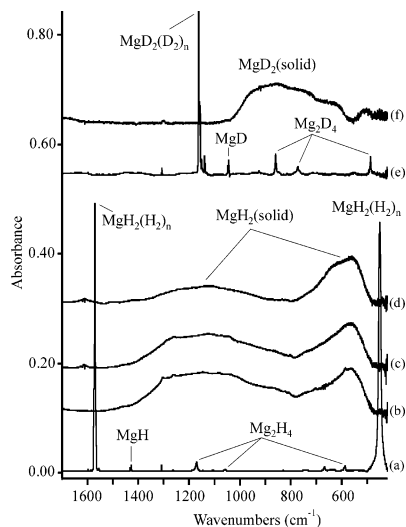*J. Phys. Chem. A, Vol. 108, No. 52, 2004* **11513**

Figure 3. Infrared spectra in the $1700-420$ cm^{-1} region for laser-ablated Mg co-deposited with hydrogen at 3.8 K: (a) after deposition with H_2 for 20 min and $240-380$ nm irradiation for 20 min, (b) after warming to 10 K, (c) after warming to 200 K, (d) after warming to 300 K, (e) after co-deposition with D_2 for 20 min and $\lambda > 240$ nm irradiation for 20 min, and (f) after warming to 50 K.
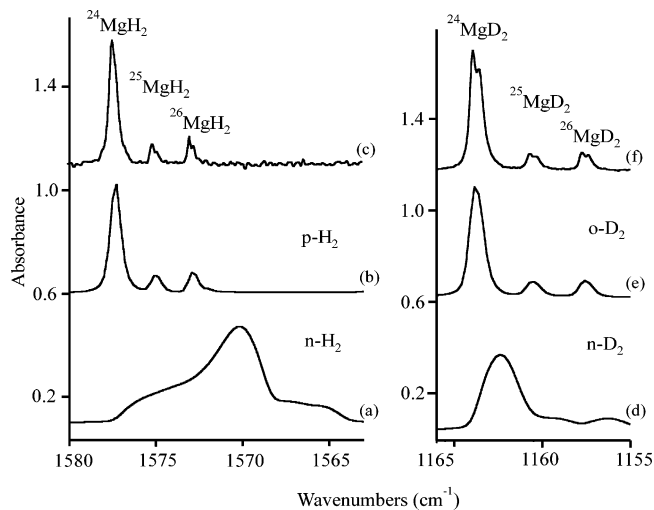

Figure 4. Infrared spectra of MgH_2 and MgD_2 in solid molecular hydrogens after $\lambda > 240$ nm irradiation at 3.8 K: (a) MgH_2 in n-H_2, (b) MgH_2 in p-H_2 (99%), (c) MgH_2 in p-H_2 (99%), 0.13 cm^{-1} resolution, (d) MgD_2 in n-D_2, (e) MgD_2 in o-D_2 (98%), and (f) MgD_2 in o-D_2 (98%), 0.13 cm^{-1} resolution.

ment region), and group B bands shift to 859.9, 772.3, and 486.5 cm^{-1} as shown in Figure 2. All other weak bands observed in solid hydrogen shift in solid deuterium as listed in Table 1. Analogous absorptions from ^{26}Mg atom reactions with H_2 in solid normal hydrogen and D_2 in solid normal deuterium gave small red-shifts as expected.

After warming above 8 K, the H_2 host evaporates and broad bands centered at 1160 and 560 cm^{-1} appear on the cold window. Spectra recorded at 10, 200, and 300 K (Figure 3b,c,d) reveal band broadening with increasing temperature. Spectra for an analogous deuterium sample give a broad counterpart centered at 880 cm^{-1} (Figure 3f).

The absorptions for reaction products of magnesium atom with H_2 in parahydrogen are also listed in the Table 1. The interaction in solid parahydrogen is reduced, the band contours are much sharper than in normal solid hydrogen,[25] and natural magnesium isotopic splittings are resolved. In addition the absorptions show slight blue-shifts in both p-H_2 and o-D_2. Figure
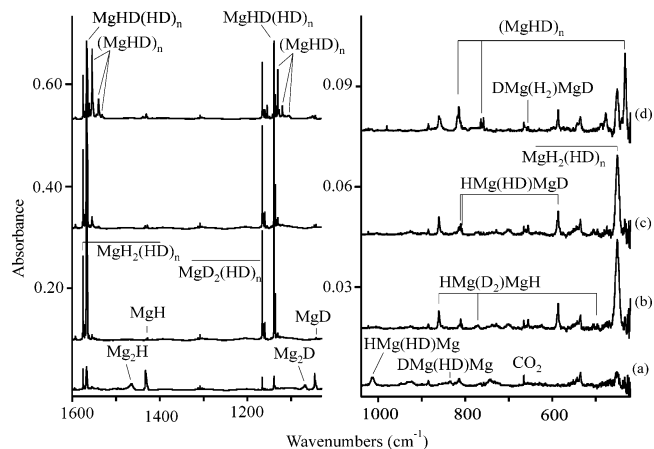

Figure 5. Infrared spectra in selected regions for laser-ablated Mg co-deposited with HD at 3.8 K: (a) after deposition for 20 min, (b) after $240-380$ nm irradiation for 20 min, (c) after annealing to 8 K, and (d) after annealing to 9 K.

4 compares spectra in different nuclear spin isomers. Spectra recorded at 1/8 cm^{-1} resolution revealed site splittings about 0.3 cm^{-1} lower than the main magnesium isotopic peaks.

Infrared spectra for Mg in pure HD give sharp bands in both Mg-H and Mg-D stretching regions, as shown in Figure 5. An experiment was done with $H_2 + D_2$ (50−50) and the strong 1570.3 and 1162.2 cm^{-1} bands after $240-380$ nm irradiation were 0.28 and 0.089 absorbance units, respectively, and weaker 1431.6 and 1045.9 cm^{-1} bands were 0.024 and 0.011 absorbance units.

The neon matrix spectra of reaction products of magnesium and molecular hydrogen are shown in Figure 6, and absorptions are listed in Table 2. The major absorptions at 1431.3 cm^{-1} and at 1574.0 and 450.4 cm^{-1} (group A) appeared on the Mg atom reaction with H_2 in excess neon during deposition. On $\lambda > 240$ nm photolysis group B bands were generated while group A bands increased markedly. On annealing to 9.5 K new bands at 1564.5 and 1551.6 cm^{-1} appeared and increased on further annealing. New absorptions with deuterium and deuterium hydride reagents are listed in Table 2.

Calculations. The linear structure of MgH_2 has been calculated with different theoretical methods.[7,26−28] By using B3LYP and MP2 the Mg−H bond length is predicted to be 1.701 and 1.704 Å, respectively, which are in very good agreement with the recent gas-phase value of 1.7033 Å.[6] The linear MgH_2 molecule is polarized to be $H^{\delta-}-Mg^{\delta+}-H^{\delta-}$, and as a result molecular hydrogen can be associated to $H^{\delta-}$ and $Mg^{\delta+}$ to form a large cluster. The coplanar $MgH_2(H_2)_4$ model complex is predicted to be stable local minimum with two H_2 are attached to the end $H^{\delta-}$ and the other two H_2 to $Mg^{\delta+}$. Apparently the interactions are slightly different, namely $H^{\delta-}\cdots HH$ is 2.740 Å while $Mg^{\delta+}\cdots H_2$ is 2.867 Å. The D_{4h} $MgH_2(H_2)_6$ model complex forms an even more stable local minimum, and the ligand distances decrease to 2.731 and 2.825 Å. Solid hydrogen is a perfect medium to study this cluster in which MgH_2 is trapped and infrared modes of H_2 attached to MgH_2 are activated. Tables 3 and 4 give the results of our calculations.

$Mg(H_2)^+$ and MgH_2^+ are calculated and $Mg(H_2)^+$ lies 46.6 kcal/mol lower at the B3LYP level. The strong H−H stretching mode should be detected if Mg^+ generated from laser ablation is trapped in solid hydrogen. Similar cations $M(H_2)^+$ have been calculated and observed for group 3A metals.[10−14] The MgH_2^- anion is bent and the electron affinity for MgH_2 is predicted to be only 4.7 kcal/mol.
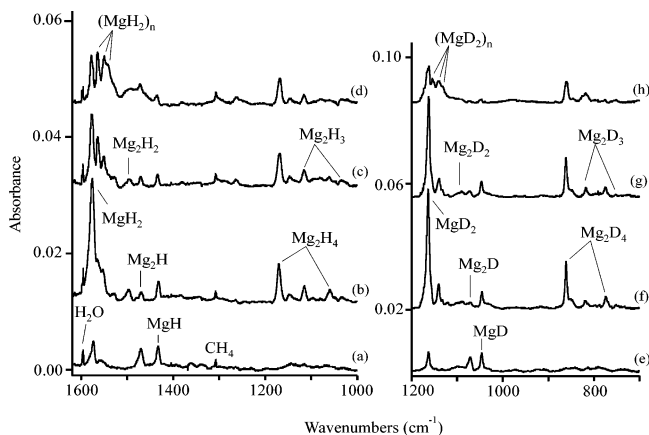
11514 *J. Phys. Chem. A, Vol. 108, No. 52, 2004*

Wang and Andrews

Figure 6. Infrared spectra for laser-ablated Mg in the 1620−1000 cm^{-1} region with Ne/H$_2$ and in the 1200−700 cm^{-1} region with Ne/D$_2$: (a) after deposition with 4% H$_2$ in neon for 60 min, (b) after $\lambda > 240$ nm irradiation for 20 min, (c) after annealing to 9 K, and (d) after annealing to 12 K, (e) after deposition with 4% D$_2$ in neon for 60 min, (f) after $\lambda > 240$ nm irradiation for 20 min, (g) after annealing to 9 K, and (h) after annealing to 13 K.
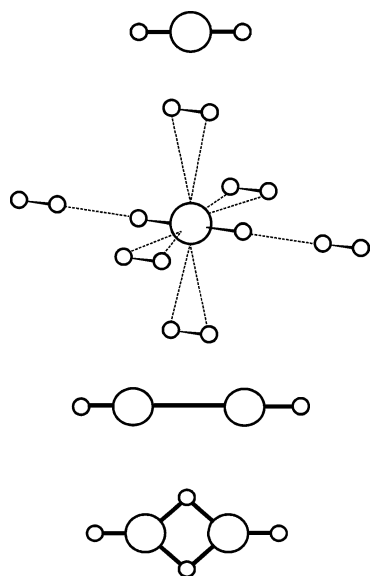

Figure 7. Calculated structures for MgH$_2$, MgH$_2$(H$_2$)$_6$, Mg$_2$H$_2$, and Mg$_2$H$_4$. Bond lengths and angles given in Table 3.
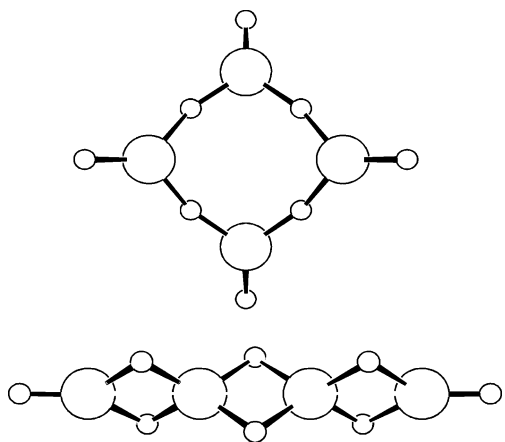

Figure 8. Calculated structures for cyclic and chain Mg$_4$H$_8$ isomers. Bond lengths and angles given in Table 3.

The dimer of MgH$_2$, HMg(μ-H)$_2$MgH, has been theoretically investigated[29] and the doubly bridged planar D_{2h} structure has

TABLE 2: Infrared Absorptions (cm^{-1}) Observed from Reactions of Magnesium and Dihydrogen in Excess Neon

H$_2$/Ne	D$_2$/Ne	HD/Ne	identification
1583.7			Mg$_2$H$_4$
1576.8	1163.2	1569.3, 1140.7	MgH$_2$ (phot)
1574.0	1162.4	1569.3, 1140.7	MgH$_2$ (dep)
1564.5	1140.6	1558.2, 1132.7	Mg$_3$H$_6$
1551.6	1140.6	1544.9, 1123.6	Mg$_4$H$_8$
1496.4	1088.9	1508.9, 1099.3	Mg$_2$H$_2$
1470.0	1070.9	1470.0, 1070.9	Mg$_2$H
1431.3	1046.2	1431.3, 1046.2	MgH
1169.9	860.8	1167.7, 862.1	Mg$_2$H$_4$
1114.6	818.5		Mg$_2$H$_3$
1058.9	773.6	761.5	Mg$_2$H$_4$
665.9	486.3		Mg$_2$H$_4$
450.4			MgH$_2$

the lowest energy. Our B3LYP and MP2 calculations reach the same conclusions. Higher polymers Mg$_3$H$_6$ and Mg$_4$H$_8$ were calculated at the B3LYP level and slightly higher energy single-bridged (s-Mg$_3$H$_6$ and s-Mg$_4$H$_8$) and lower energy double-bridged (d-Mg$_3$H$_6$ and d-Mg$_4$H$_8$) hydrogen bonds were obtained. The double-bridged hydrogen bond lengths and bond angles are basically very close to Mg$_2$H$_4$, suggesting strong Mg−H−Mg stretching modes should be observed if such molecules are trapped in the matrix. However the single-bridged hydrogen bond lengths are shorter and angles are much larger, and the strongest IR absorptions are located in the Mg−H stretching region. Figures 7 and 8 compare several calculated structures.

Analogous calculations were done for MgH, Mg$_2$H radical, Mg$_2$H$_2$, and Mg$_2$H$_3$ radical. For the ground-state MgH 1.742 Å bond lengths and a 1461.6 cm^{-1} Mg−H stretching frequency are computed, which are very close to recent gas-phase experimental values of 1.7298 Å and 1431.98 cm^{-1}, respectively.[30] MP2 calculations give similar results. Two Mg$_2$H radical structures are located: MgMgH is lower than MgHMg by 2.6 kcal/mol. Two isomers of MgH dimer are found, and linear HMgMgH lies 10.5 kcal/mol lower in energy than rhombic Mg(μ-H)$_2$Mg. For the Mg$_2$H$_3$ radical, single-bridged (s-Mg$_2$H$_3$) and double-bridged (d-Mg$_2$H$_3$) isomers are located on the potential energy surface. The d-Mg$_2$H$_3$ is 13.3 kcal/mol lower in energy and characterized by the strongest Mg−H−Mg stretching mode, but s-Mg$_2$H$_3$ with higher energy shows the strongest Mg−H stretching mode.

Discussion

Infrared spectra of magnesium hydrides and dihydrogen complexes will be assigned on the basis of isotopic shifts and agreement with density functional calculations.

MgH$_2$. In solid neon the 1574.0 cm^{-1} band increased markedly on 240 nm photolysis and shifted to 1576.8 cm^{-1} (Figure 6), which tracks the 450.4 cm^{-1} absorption. These two bands can be assigned to Mg−H stretching and H−Mg−H bending modes of MgH$_2$ for the following reasons. The deuterium counterpart for the 1576.8 cm^{-1} band was found at 1163.2 cm^{-1}, giving a 1.3556 H/D isotopic frequency ratio, which is appropriate for the Mg−H stretching mode, but 450.4 cm^{-1} shifts out of our measurement region. With HD in neon two new strong bands at 1569.3 cm^{-1} in the Mg−H stretching region and at 1140.7 cm^{-1} in the Mg−D stretching region (H/D = 1.3756) were observed on 240 nm photolysis. The relationship of the HD product absorptions and the MgH$_2$ and MgD$_2$ bands demonstrates that two equivalent H(D) atoms are involved in the vibration and that an unobserved stretching mode appears at lower frequency. In solid argon the MgH$_2$ absorptions were observed at 1571.9 and 439.8 cm^{-1}.[7] The antisymmetric

Magnesium Hydrides, Complexes, and Dihydrides

J. Phys. Chem. A, Vol. 108, No. 52, 2004 **11515**

TABLE 3: Magnesium Hydride Geometries, Vibrational Frequencies (cm⁻¹), and Intensities Calculated at the B3LYP/6-311++G(3df,3pd) Level of Theory

species	structure[a]	E[b]	frequencies, cm⁻¹ (intensities, km/mol)
MgH ($^2\Sigma$)	MgH: 1.742	0.0	MgH: 1461.6 (252)
			MgD: 1054.5 (131)
MgH⁻ ($^1\Sigma$)	MgH: 1.877		MgH⁻: 1088.4 (2325)
			MgD⁻: 785.3 (1151)
MgH₂ ($^1\Sigma_g^+$)	MgH: 1.701	0.0	MgH₂: 1637.3 (σ_u, 440), 1613.2 (σ_g, 0), 428.3 (π_u, 472 × 2)
	HMgH: 180.0		MgD₂: 1202.2 (237), 1141.2 (0), 314.5 (245 × 2)
MgH₂⁻ ($^2A_1$)	MgH: 1.782	−4.7	MgH₂⁻: 1342.3 (b₂, 689), 1327.7 (a₁, 1240), 529.3 (a₁, 1295)
	HMgH: 125.4		
Mg(H₂)⁺ ($^2A_1$)	MgH: 2.573	171.9	Mg(H₂)⁺: 4289.6 (a₁, 160), 371.9 (b₂, 17), 265.1 (a₁, 73)
	HH: 0.751		
MgH₂⁺ ($^2\Sigma_u^+$)	MgH: 1.788	218.5	MgH₂⁺: 1312.2 (σ_g, 0), 1016.5 (σ_u, 2036), 121.2 (π_u, 71 × 2)
MgH₃⁻ ($^1A_1'$)	MgH: 1.804		MgH₃⁻: 1356.3 (0), 1275.2 (e′, 945 × 2), 608.6 (e′, 495 × 2), 552.7 (a₂″, 776)
	HMgH: 120.0		
MgH₂(H₂)₄ (D_{2h})	MgH: 1.702		MgH₂(H₂)₄: 4390.4 (a_g, 0), 4390.3 (b₁ᵤ, 26), 4368.6 (a_g, 0), 4368.1 (b₂ᵤ, 5),
	MgH′: 2.857		1631.6 (b₁ᵤ, 515), 453.6 (b₂ᵤ, 541), 436.5 (b₃ᵤ, 433), ...
	H′H′: 0.745		
	HH″: 2.740		
	H″H″: 0.744		
MgH₂(H₂)₆ (D_{4h})	MgH: 1.703		MgH₂(H₂)₆: 4387.8 (a₁_g, 0), 4387.6 (a₂ᵤ, 31), 4366.8 (a₁_g, 0), 4366.3 (b₃_g, 0),
	MgH′: 2.825		4365.9 (eᵤ, 4 × 2), 1623.7 (a₂ᵤ, 520), 1605.2 (0), 459.2 (e₂ᵤ, 519 × 2), ...
	H′H′: 0.746		MgD₂(D₂)₆: 3103.9 (0), 3103.7 (15), 3089.0 (0), 3088.6 (0), 3088.4 (2 × 2), 1192.0 (275),
	HH″: 2.713		1135.5 (0), 332.8 (285 × 2), ...
	H″H″: 0.744		
MgMgH ($^2\Sigma$)	MgMg′: 3.072	0.0	MgMgH: 1506.7 (σ, 718), 185.0 (σ, 1), 128.3 (σ, 92 × 2)
	MgH: 1.734		MgMgD: 1087.5 (371), 183.2 (1), 96.7 (48 × 2)
MgHMg ($^2\Sigma^+$)	MgH: 1.951	2.6	MgHMg: 863.9 (σ_u, 1596), 309.1 (π_u, 7 × 2), 208.1 (σ_g, 0)
Mg₂H₂ ($^1\Sigma_g^+$) (linear)	MgH: 1.721	0.0	Mg₂H₂: 1572.0 (σ_g, 0), 1551.3 (σ_u, 1082), 300.5 (π_g, 0 × 2), 269.1 (σ_g, 0), 244.6 (π_u, 246 × 2)
	MgMg: 2.867		Mg₂D₂: 1135.1 (0), 1119.2 (563), 263.6 (0), 230.0 (0 × 2), 176.5 (128 × 2)
			HMg₂D: 1561.8 (525), 1127.0 (298), ...
Mg₂H₂ (^1A_g) (rhomb)	MgH: 1.915	10.5	Mg₂H₂: 1278.6 (a_g, 0), 1029.9 (b₂ᵤ, 349), 982.6 (b₃_g, 0), 700.0 (b₁ᵤ, 675), 631.8 (b₃ᵤ, 134),
	MgHMg: 95.9		316.7 (a_g, 0)
d-Mg₂H₃ ($^2A_1$) (DB)	MgH: 1.872	0.0	Mg₂H₃: 1615.2 (288), 1292.5 (81), 1162.2 (1047), 1042.8 (451), 1025.9 (70), 596.0 (162),
	Mg′H: 1.905		336.3 (117), 322.5 (3), 229.4 (153)
	MgH′: 1.700		Mg₂D₃: 1165.9 (182), 917.7 (52), 836.4 (515), 753.8 (239), 732.2 (36), 434.8 (93), 318.5 (3),
			250.8 (61), 169.0 (78)
s-Mg₂H₃ ($^2A_1$) (SB)	MgH: 1.878	13.3	Mg₂H₃: 1623.1 (1), 1610.5 (659), 1140.1 (245), 1060.6 (481), 348.2 (265), 275.5 (0),
	MgH′: 1.698		251.5 (18), 222.4 (23), 215.8 (253)
Mg₂H₄ (^1A_g) (D_{2h})	MgH: 1.875		Mg₂H₄: 1640.7 (a_g, 0), 1632.7 (b₁ᵤ, 418), 1308.1 (a_g, 0), 1238.9 (b₁ᵤ, 1135), 1104.6 (b₃_g, 0),
	MgH′: 1.694		1083.6 (b₂ᵤ, 630), 671.7 (b₃ᵤ, 488), 373.1 (b₂ᵤ, 347), 330.0 (a_g, 0), 311.8 (b₃_g, 0), 298.7
	MgHMg: 95.6		(b₂_g, 0), 218.8 (b₃ᵤ, 262)
			Mg₂D₄: 1185.6 (0), 1176.9 (283), 927.3 (0), 892.7 (551), 786.1 (0), 784.5 (351), 489.5 (272),
			322.3 (0), 267.7 (176), 239.7 (0), 228.8 (0), 155.9 (132)
s-Mg₃H₆	MgH: 1.697	0.0	Mg₃H₆: 1646.1 (e′, 85 × 2), 1633.1 (a₁′, 0), 1599.9 (e′, 1404 × 2), 1505.9 (a₂′, 0), 935.8
	MgH′: 1.828		(a₁′, 0), 798.6 (e′, 619 × 2), 629.8 (a₂″, 795), 406.7 (e″, 0 × 2), ..., 147.7 (e″, 0 × 2)
	MgH′Mg: 139.1		
d-Mg₃H₆	MgH: 1.693	−3.8	Mg₃H₆: 1638.5 (a₁, 0), 1636.1 (b₂, 402), ..., 1204.5 (b₂, 2504), 1078.2 (e, 456 × 2), 654.9
	MgH′: 1.862		(e, 290 × 2), ..., 68.2 (e, 13 × 2)
	MgH′Mg: 94.0		
s-Mg₄H₈	MgH: 1.698	0.0	Mg₄H₈: 1769.4 (b₂, 116), 1730.8 (e, 1208 × 2), 1632.8 (a₁, 0), 1618.1 (e, 878 × 2), 1616.7
	MgH′: 1.814		(b₂, 199), 1615.3 (a₂, 0), 756.6 (a₁, 0), 642.4 (e, 979 × 2), 618.1 (b₂, 998), ..., 21.5 (a₁, 0)
	MgH′Mg: 163.3		
d-Mg₄H₈	MgH: 1.694	−12.7	Mg₄H₈: 1637.6 (a_g, 0), 1636.5 (b₃ᵤ, 402), 1178.5 (b₃ᵤ, 4054), 1117.8 (b₂ᵤ, 361), ..., 1095.4
	MgH′: 1.866		(b₁ᵤ, 639), 1088.3 (b₂ᵤ, 852), ..., 38.6 (b₂ᵤ, 5)
	MgH′Mg: 94.0		

[a] Bond lengths (Å), angles (deg). [b] Relative energies of stoichiometric species (kcal/mol).

stretching mode of MgH₂ was measured in the gas phase at 1586.7 cm⁻¹ and MgD₂ at 1176.5 cm⁻¹, which gives a slightly lower H/D frequency ratio.[6] The gas and argon measurements bracket our neon matrix value.

Calculation with B3LYP/6-311++G(3df,3pd) gave MgH₂ with a linear structure and a strong Mg−H antisymmetric stretching mode at 1637.3 cm⁻¹ (σ_u) and a bending mode at 428.3 cm⁻¹ (π_u), which reproduce experimental observations. We expect that the bending mode will appear around 460 cm⁻¹ in the gas-phase molecule.

MgH₂(H₂)ₙ. In solid, normal hydrogen bands at 1569.5 cm⁻¹ (site splitting at 1576.4 cm⁻¹) (Mg−H stretching) and 450.1 cm⁻¹ (H−Mg−H bending) appeared on deposition and in-

creased by 6-fold on 240−380 nm photolysis. A sharp band at 3078.8 cm⁻¹ tracks the 1569.5 cm⁻¹ band and must be the overtone of the Mg−H stretching mode. The 3078.8 cm⁻¹ band is 60.2 cm⁻¹ less than 1569.5 × 2 = 3139.0 cm⁻¹, which is appropriate for anharmonicity. In solid parahydrogen, analogous strong bands observed at 1577.4 and 450.4 cm⁻¹, and an overtone at 3091.6 cm⁻¹ show slight blue-shifts. The deuterium counterpart was found at 1161.4 cm⁻¹ (site splitting at 1163.2 cm⁻¹) in pure normal D₂ and at 1163.7 cm⁻¹ in ortho D₂. In pure HD two strong bands at 1567.2 and 1139.1 cm⁻¹ were observed. Comparing neon spectra, these bands are appropriate for MgH₂, MgD₂, and MgHD. However, in pure H₂ two bands at 4139.0 and 4114.5 cm⁻¹ near the H₂ fundamental track the

TABLE 4: Calculated Geometries, Vibrational Frequencies (cm⁻¹), and Intensities at the MP2/6-311++G(3df,3pd) Level

| species	structure (Å, deg)	frequencies, cm⁻¹ (intensities, km/mol)
MgH ($^2\Sigma$)	MgH: 1.729	MgH: 1556.2 (368)
		MgD: 1122.8 (191)
MgH$_2$ ($^1\Sigma_g^+$)	MgH: 1.704	MgH$_2$: 1659.4 (σ_u, 465), 1639.1 (σ_g, 0), 441.5 (π_u, 568 × 2)
	HMgH: 180.0	MgD$_2$: 1218.4 (251), 1159.5 (0), 324.1 (306 × 2)
MgH$_2$(H$_2$)$_4$ ($^1A_1$)	MgH: 1.705	MgH$_2$(H$_2$)$_4$: 4494.7 (0), 4494.5 (22), 4463.9 (0), 4463.4 (9), 1655.3 (534), 1637.5 (0), 474.4 (615),
	HMgH: 180	442.4 (522), ...
	MgH′: 2.780	
	H′H′: 0.740	
	HH″: 2.687	
	H″H″: 0.738	
MgMgH ($^2\Sigma$)	MgMg′: 3.072	MgMgH: 1651.5 (σ, 317), 383.2 (π, 4 × 2), 319.7 (σ, 50), 296.6 (π, 115 × 2)
	MgH: 1.734	MgMgD: 1119.0 (185), 286.3 (1 × 2), 316.5 (53), 221.6 (54 × 2)
Mg$_2$H$_2$ ($^1\Sigma_g^+$)	MgH: 1.721	Mg$_2$H$_2$: 1601.9 (σ_g, 0), 1581.4 (σ_u, 1078), 312.3 (π_g, 0 × 2), 275.6 (σ_g, 0), 258.6 (π_u,290 × 2)
	MgMg: 2.893	Mg$_2$D$_2$: 1156.6 (0), 1141.0 (561), 269.9 (0), 238.7 (0 × 2), 186.6 (151 × 2)
d-Mg$_2$H$_3$ ($^2A_1$)	MgH: 1.704	Mg$_2$H$_3$: 1641.0 (a$_1$, 279), 1321.9 (a$_1$, 190), 1218.9 (a$_1$, 1230), 1070.3 (b$_2$, 57), 1054.6 (b$_2$, 517),
	MgH′: 1.872	606.5 (b$_1$, 154), 344.6 (b$_2$, 142), 329.7 (a$_1$, 3), 244.5 (b$_1$, 195)
	Mg′H′: 1.904	
	MgMg′: 2.828	
Mg$_2$H$_4$ (^1A_g)	MgH: 1.877	Mg$_2$H$_4$: 1660.9 (a$_g$, 0), 1652.3 (446), 1331.9 (a$_g$, 0), 1281.0 (b$_{1u}$, 1220), 1141.4 (b$_{3g}$, 0),
	MgH′: 1.699	1097.1 (b$_{2u}$, 701), 687.1 (b$_{3u}$, 579), 377.2 (b$_{2u}$, 414), 335.0 (a$_g$, 0), 320.2 (b$_{3g}$, 0), 301.6 (b$_{2g}$, 0),
	MgHMg: 96.1	225.1 (b$_{3u}$, 312)
		Mg$_2$D$_4$: 1200.1 (0), 1190.8 (308), 944.2 (0), 923.2 (588), 812.7 (0), 794.3 (391), 500.7 (322), ...

1569.5 cm⁻¹ band, and these bands are due to H−H stretching vibrations perturbed by HMgH. In solid D$_2$ analogous bands were observed at 2977.2 and 2959.5 cm⁻¹ and in solid HD at 3620.0 and 3597.6 cm⁻¹. Clearly MgH$_2$ is coordinated by surrounding H$_2$ molecules in solid hydrogen. In addition ^{26}Mg reaction with H$_2$ gave slightly red-shifted bands at 1565.2 and 449.0 cm⁻¹ and the overtone at 3073.0 cm⁻¹. Finally, the sharp natural Mg-isotopic splittings observed on annealing to 8.0 K show that a single Mg atom is involved in this product species.

The H/D isotopic frequency ratios for MgH$_2$/MgD$_2$ in the normal solids (1.3493) and the $J = 0$ solids (1.3555) are slightly different, but the latter matches the ratio in solid neon and the former is almost the same as the gas-phase isotopic frequency ratio.

Identification of the MgH$_2$ complex is further supported by quantum chemical calculations. As H$_2$ molecules are added to MgH$_2$, two different interactions are obtained, namely side-on H$_2$ to Mg and end-on H$_2$ to H. A MgH$_2$(H$_2$)$_6$ model complex calculated with the B3LYP functional, Figure 7, is a local minimum with end-on H$_2$ bonds slightly stronger than side-on H$_2$. As a result two different H−H stretching modes at 4387.6 and 4365.9 cm⁻¹ are obtained. The two H−H stretching modes are predicated 19.7 and 41.5 cm⁻¹ lower than that of free H$_2$, which are basically what is observed in solid hydrogen. In normal hydrogen two new H−H stretching frequencies at 4139.0 and 4114.5 cm⁻¹ are 13.8 and 38.3 cm⁻¹ below the solid H$_2$ fundamental (4152.8 cm⁻¹). MP2 calculations gave analogous results for MgH$_2$(H$_2$)$_4$, but the frequency calculation failed to converge for MgH$_2$(H$_2$)$_6$. Of course for MgH$_2$ trapped in a solid H$_2$ lattice even more H$_2$ molecules surround and stabilize the first shell MgH$_2$(H$_2$)$_6$ complex. Unfortunately, this complex decomposes when the hydrogen matrix evaporates and solid MgH$_2$ forms.

The insertion reaction of Mg into H$_2$ is endothermic by 4.1 kcal/mol from B3LYP and 2.9 kcal/mol from MP2 calculations. The insertion of ground-state Mg (3s,^{1}S) into H$_2$ is greatly inhibited by a large energy barrier, but the yield of MgH$_2$ increases greatly on 240 nm photolysis, so the Mg atom must be excited to the electronic state (3s3p, ^{1}P) by 240 nm to surmount the energy barrier and insert into H$_2$. In fact MgH$_2$ was observed on deposition since on laser ablation strong Mg (^{1}P → ^{1}S) emission at 284 nm was recorded in this experiment,

and MgH$_2$ is generated and trapped in the matrix.

$$Mg^* + H_2 \rightarrow MgH_2 \, (^1\Sigma_g^+) \qquad (1)$$

$$MgH_2 \, (^1\Sigma_g^+) + nH_2 \rightarrow MgH_2(H_2)_n \qquad (2)$$
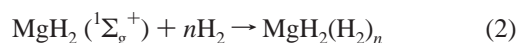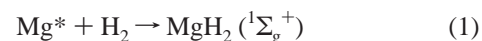
Mg$_2$H$_4$. The bands at 1587.6, 1170.5, 1058.7, and 667.2 cm⁻¹ track together in solid normal hydrogen and blue shift several wavenumbers in solid parahydrogen (Table 1). As shown in Figure 1 these bands were barely observed after deposition (trace a) but increased on $\lambda > 320$ nm photolysis and increased greatly on 240−380 nm irradiation. However, $\lambda > 240$ nm broad-band photolysis reduced these bands by 30%, but 240−380 nm irradiation restored them totally. Since MgH$_2$ increased markedly and dimerization of MgH$_2$ is feasible under these conditions, we can assign these bands to Mg$_2$H$_4$. The 1587.6 cm⁻¹ band is slightly higher than the Mg−H stretching mode of MgH$_2$, which is appropriate for the terminal Mg−H stretching mode in Mg$_2$H$_4$. The 1170.5 and 1058.7 cm⁻¹ bands are located in the bridge bond stretching region and Mg(μ-H)$_2$Mg bridge-bond stretching modes are suggested. Recall the vibrations of the Al(μ-H)$_2$Al moiety in dialane Al$_2$H$_6$:[9,10] The 1170.5 and 1058.7 cm⁻¹ bands are due to antisymmetric stretching modes parallel and perpendicular, respectively, to the Mg−Mg axis. The 667.2 cm⁻¹ band arises from bending of bridge and terminal hydrogen atoms.

In solid normal deuterium 859.9, 772.3, and 486.5 cm⁻¹ bands show the same photochemical behavior and must be assigned to Mg$_2$D$_4$. Similar experiments were done with orthodeuterium and these bands exhibit several wavenumber blue shifts. It is easy to assign the 859.9 and 772.3 cm⁻¹ bands to Mg(μ-D)$_2$-Mg motion and the 486.5 cm⁻¹ band as a bending mode in this molecule. Unfortunately the terminal Mg−D stretching mode for Mg$_2$D$_4$ is not observed since larger isotopic shift for this mode red-shifts it under the Mg−D stretching vibration of MgD$_2$.

The assignment of Mg$_2$H$_4$ is nicely supported by theoretical calculations. The most stable structure for the dimer of MgH$_2$ is the dihydrogen bridge linkage H−Mg(μ-H)$_2$Mg−H. The four strongest IR active modes calculated at the B3LYP/6-311++G-(3df,3pd) level of theory are 1632.7 (b$_{1u}$), 1238.9 (b$_{1u}$), 1083.6 (b$_{2u}$), and 671.7 (b$_{3u}$) cm⁻¹, which overestimate by 2.8%, 5.8%, 2.4%, and 0.7%, respectively, our observed frequencies. These

Magnesium Hydrides, Complexes, and Dihydrides

J. Phys. Chem. A, Vol. 108, No. 52, 2004 **11517**

are typical deviations for the B3LYP functional used in frequency calculations of main group light metal hydrides.[9,10] Similar MP2 frequency calculations give four strong modes at 1652.3, 1281.0, 1097.1, and 687.1 cm^{-1}, which are slightly higher than the B3LYP values, and comparable to values given in the previous report.[29]

Corresponding experiments were done with Mg and pure HD and diagnostic bands for the identification of H$-$Mg(μ-H)$_2$Mg$-$H are observed. Three isotopomers are possible for the doubly D-substituted molecule, H$-$Mg(μ-HD)Mg$-$D, H$-$Mg-(μ-D)$_2$Mg$-$H, and D$-$Mg(μ-H)$_2$Mg$-$D, using the HD reagent, and very complicated spectra are thus expected. However, some isotopomers may be disfavored because of higher zero-point energies (ZPE). In the Mg$-$H stretching region new 1594.0 and 1592.6 cm^{-1} absorptions were observed in Mg + HD spectra and in the bending region 586.3 and 505.3 cm^{-1} bands appeared with the upper bands. A set of bands at 1169, 1145.0, 860.8, 811.0, 807.9, and 771.1 cm^{-1} track bands mentioned above and must be due to a common molecular species. In this case theoretical calculations are extremely helpful to make specific assignments. First, H$-$Mg(μ-D)$_2$Mg$-$H is the most favorable molecule at low temperature because of the lowest ZPE of all three isotopomers while D$-$Mg(μ-H)$_2$Mg$-$D is the highest. Second, the calculated frequencies for the Mg(μ-D)$_2$Mg subunit in H$-$Mg(μ-D)$_2$Mg$-$H are very close to this subunit in D$-$Mg-(μ-D)$_2$Mg$-$D and likewise H$-$Mg(μ-H)$_2$Mg$-$H is a good model for the Mg(μ-H)$_2$Mg subunit in D$-$Mg(μ-H)$_2$Mg$-$D. Two new bands observed at 860.8 and 771.1 cm^{-1} match the frequencies for the Mg(μ-D)$_2$Mg subunit. In addition the 1592.6 cm^{-1} band is appropriate for the Mg$-$H mode and the 505.3 cm^{-1} band for the bending mode. Hence, these bands are assigned to H$-$Mg(μ-D)$_2$Mg$-$H. B3LYP calculation gave IR active bands at 1632.1, 893.5, 788.5, and 509.6 cm^{-1}, which reproduced experimental values very well. Third, the calculated vibrational modes for the Mg(μ-HD)Mg subunit (B3LYP) in H$-$Mg(μ-HD)Mg$-$D are split to 1219.2 and 1180.8 cm^{-1} in the upper hydrogen region, and to 835.1 and 830.5 cm^{-1} in the lower deuterium region, which match the observed 1169, 1146.3, and 811.0, 807.9 cm^{-1} absorptions. In addition new 1594.0 and 1145.0 cm^{-1} bands are due to the Mg$-$H and Mg$-$D stretching modes and the 586.3 cm^{-1} band is due to the bending mode for this molecule, which are computed at 1636.6, 1180.7, and 588.4 cm^{-1}, respectively. Fourth, weak absorptions were observed for the higher energy D$-$Mg(μ-H)$_2$Mg$-$D isotopomer at 1204.9 and 655.5 cm^{-1}. Hence we conclude the Mg$_2$H$_2$D$_2$ isotopic identifications and the H$-$Mg(μ-H)$_2$Mg$-$H assignment.
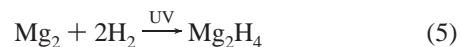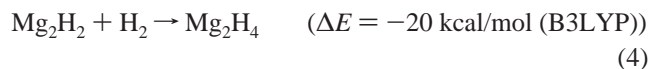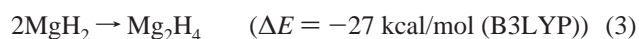
In the experiment with H$_2$ + D$_2$ (50$-$50) MgH$_2$ and MgD$_2$ were produced in an approximately 2/1 ratio based on calculated isotopic intensities. Hence, their dimerization could produce Mg$_2$H$_4$ as well as Mg$_2$H$_2$D$_2$ in favorable yield. The 1587.1 and 1169.8 cm^{-1} bands in this experiment are due to H$-$Mg(μ-H)$_2$Mg$-$H and the 860.5 cm^{-1} band must be due to D$-$Mg-(μ-D)$_2$Mg$-$D. The strongest band (835 cm^{-1}) for H$-$Mg(μ-HD)MgD is not observed yet this isotopomer is the only mixed dimer of MgH$_2$ and MgD$_2$, so other mechanisms must be considered.

The absorptions of H$-$Mg(μ-H)$_2$Mg$-$H were also found in solid neon. Laser ablated Mg atom reaction with H$_2$ in excess neon generates MgH$_2$ monomer. With 240 nm photolysis the yield of MgH$_2$ increased 10-fold, and meanwhile new bands were produced at 1583.7, 1169.9, 1058.9, and 665.9 cm^{-1}. These bands are appropriate for the H$-$Mg(μ-H)$_2$Mg$-$H molecule based on comparison with observations in solid hydrogen. With D$_2$ in solid neon these bands shift to 1173.8, 860.8, 773.6, and

486.5 cm^{-1}. Experiments with Mg reaction HD in solid neon gave absorptions of H$-$Mg(μ-D)Mg$-$H at 862.1, 773.6, and 506.2 cm^{-1}, and for H$-$Mg(μ-HD)Mg$-$D at 1168.3, 812.5, and 589.7 cm^{-1}. Some weak bands for this isotopomer were not observed because of band broadness in solid neon.

The absorptions of H$-$Mg(μ-H)$_2$Mg$-$H in solid argon were tentatively assigned in our early work,[7] and the strongest of these at 1164.2 cm^{-1} is confirmed by comparison with our neon matrix absorptions. However, the solid argon matrix is more rigid and polarizable, and the dimerization of MgH$_2$ is strongly inhibited. As a result the yield of H$-$Mg(μ-H)$_2$Mg$-$H is very small. A similar case was found for the Al atom reaction with H$_2$: we trapped H$_2$-Al(μ-H)$_2$Al$-$H$_2$ in large yield in solid hydrogen and neon, but only very weak absorptions were observed in solid argon.[10]

The Mg$_2$H$_4$ molecule could in principle be formed from dimerization of either MgH$_2$ or Mg$_2$H$_2$ adding H$_2$ to give Mg$_2$H$_4$. Spontaneous formation of Mg$_2$H$_4$ is observed on annealing suggesting that no significant activation energy is required for exothermic reaction 3. This is in agreement with the spontaneous formation of solid MgH$_2$ on evaporation of the solid H$_2$ matrix.

$$2MgH_2 \rightarrow Mg_2H_4 \qquad (\Delta E = -27 \text{ kcal/mol (B3LYP)}) \quad (3)$$

$$Mg_2H_2 + H_2 \rightarrow Mg_2H_4 \qquad (\Delta E = -20 \text{ kcal/mol (B3LYP)}) \quad (4)$$

$$Mg_2 + 2H_2 \xrightarrow{\text{UV}} Mg_2H_4 \quad (5)$$

Some of the MgH$_2$ molecules from reaction 1 with high vibrational energy before relaxation can surmount the energy barrier to dimerize (reaction 3). The Mg$_2$H$_2$ molecules trapped in solid hydrogen after deposition could react with H$_2$ to give Mg$_2$H$_4$ through $\lambda > 320$ nm photolysis; however, $\lambda > 290$ nm and 240$-$380 nm irradiation gives far more Mg$_2$H$_4$ after Mg$_2$H$_2$ is gone.
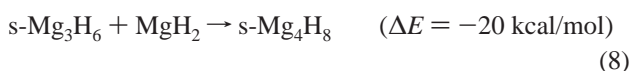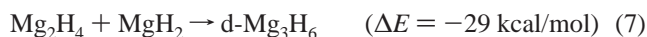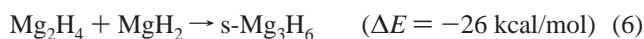
Laser-ablated and excited Mg that does not react must relax to the ground ^1S_o state, which will not react with H$_2$, but will dimerize to Mg$_2$ as observed previously. This Mg$_2$ species absorbs strongly at 370 nm,[31] and Mg$_2$* reacts in the hydrogen matrix cage to give Mg$_2$H$_4$, reaction 5.

Mg$_3$H$_6$ and Mg$_4$H$_8$. In solid neon new bands at 1564.5 and 1551.6 cm^{-1} appeared on 240 nm photolysis and increased on further annealing to 10$-$12 K. With D$_2$ in solid neon the two bands shift to 1154.2 and 1140.6 cm^{-1} and with HD in neon at 1558.2 and 1544.9 cm^{-1} (Mg$-$H stretching), and 1132.7 and 1123.6 cm^{-1} (Mg$-$D stretching). Similar broad bands were also observed in solid H$_2$, D$_2$, and HD. The photolysis and annealing behaviors of these bands led us to consider higher polymer assignment.

DFT calculations were performed for Mg$_3$H$_6$ and Mg$_4$H$_8$, and single-bridged (cyclic)-Mg(H)$-$H$-$ and double-bridged (chain) $-$Mg-(μ-H)$_2-$ molecules converged (Figure 8). Although these two conformers have very close energies, the strongest IR active modes are very disparate based on single or double bridged metal$-$hydrogen$-$metal bonds. The single-bridged conformers show a much shorter bridged Mg$-$H bond than double bridged and as a result the vibration stretching mode of bridged Mg$-$H strongly couples with end Mg$-$H stretching motion. It is not surprising that the frequency for this mode is very close to Mg$-$H stretching in free MgH$_2$. However, for double-bridged conformers the bridged Mg$-$H bond is very close to the MgH$_2$ dimer HMg$-$(μ-H)$_2-$MgH and the strongest IR active modes are in the same region as observed for the MgH$_2$ dimer. As

shown in Table 3 very strong absorptions at 1599.9 cm^{-1} for s-Mg$_3$H$_6$ and at 1730.8 and 1618.1 cm^{-1} for s-Mg$_4$H$_8$ (s denotes single bridge) are calculated with the B3LYP functional, which basically agree with the observed 1564.5 and 1551.6 cm^{-1} bands. Several weak absorptions below these two bands appeared on annealing to higher temperature, which must be due to higher polymers with single bridged bond linkage. However, the calculated strong absorptions at 1204.5 cm^{-1} for d-Mg$_3$H$_6$ and 1178.5 cm^{-1} for d-Mg$_4$H$_8$ (d denotes double bridge) are not observed. It is very interesting to note in contrast that double bridged beryllium hydride polymer has been identified in solid hydrogen, which will be discussed in an upcoming paper.

The polymerization of MgH$_2$ is exothermic based on our initial calculations and this is the reason the bulk MgH$_2$ is very stable and the decomposition temperature is very high (360 °C).[2] As we observed in both solid hydrogen and neon s-Mg$_3$H$_6$ is trapped instead of d-Mg$_3$H$_6$ although the later is more exothermic. Higher polymers are obtained in the same way. It appears from the spectrum of the solid that higher 3-dimensional polymers revert to the double-bridged model.

$$\text{Mg}_2\text{H}_4 + \text{MgH}_2 \rightarrow \text{s-Mg}_3\text{H}_6 \quad (\Delta E = -26 \text{ kcal/mol}) \quad (6)$$

$$\text{Mg}_2\text{H}_4 + \text{MgH}_2 \rightarrow \text{d-Mg}_3\text{H}_6 \quad (\Delta E = -29 \text{ kcal/mol}) \quad (7)$$

$$\text{s-Mg}_3\text{H}_6 + \text{MgH}_2 \rightarrow \text{s-Mg}_4\text{H}_8 \quad (\Delta E = -20 \text{ kcal/mol})$$
$$(8)$$

MgH$_2$ Solid. Warming the previously described hydrogen samples to 10 K allowed the hydrogen host to evaporate, the MgH$_2$(H$_2$)$_n$ complexes to decompose, and a solid magnesium hydride film to form on the CsI substrate. This film exhibited broad 1160 and 560 cm^{-1} absorptions (Figure 3) and remained on the support at room temperature. The deuterium counterpart exhibited a broad 880 cm^{-1} absorption (H/D ratio 1.32).

The vibrational spectrum of solid magnesium hydride determined from neutron scattering contains broad bands at 72, 124, and 148 meV (580, 1000, and 1200 cm^{-1}).[5] Our solid MgH$_2$ film spectrum (Figure 3) reveals a broad 1000−1300 cm^{-1} flat-top band centered at 1160 cm^{-1} and a 560 cm^{-1} peak, which are in excellent agreement with the vibrational density of states from neutron scattering.[5] It appears that we have formed a solid MgH$_2$ film by allowing MgH$_2$ molecules to aggregate that is similar to that formed on Mg reacting with H$_2$ gas at 500 °C.

The 1000 and 1200 cm^{-1} vibrations in solid MgH$_2$ are probably due to bridge Mg−H−Mg bond stretching modes with neon matrix counterparts near 1059 and 1170 cm^{-1} for the H−Mg(μ-H)$_2$Mg−H molecule discussed above. The 1.95 Å solid X-ray Mg−H bond length[4] is slightly longer than our B3LYP value (1.875 Å) for bridge bonds in the latter molecule. We note that calculated lattice energy using a Born−Mayer model is −2906 kJ/mol as compared to the experimental Born−Haber cycle value of −2721 kJ/mol. This difference has been attributed to an appreciable covalent contribution to the bonding.[32]

MgH and Mg$_2$H. A strong band at 1427.1 cm^{-1} with satellites at 1429.5, 1430.6, and 1431.9 cm^{-1} appeared on deposition and reaction of Mg with H$_2$ in solid normal hydrogen. This band decreased on 240−380 nm photolysis (Figure 1c), but was restored in part on 193 nm irradiation (another experiment). In solid normal deuterium the counterparts were observed at 1042.8, 1044.4, 1045.9, and 1047.5 cm^{-1}. In solid HD two sets of bands at 1428.1, 1430.6, 1431.9, and 1433.5 cm^{-1} (Mg−H stretching region) and at 1042.6, 1044.3, 1045.5,

and 1046.9 cm^{-1} (Mg−D stretching region) were obtained. This is appropriate for the diatomic MgH molecule. We note that the absorptions of Mg−H and Mg−D stretching modes in solid H$_2$, D$_2$, and HD are slightly shifted because of different interactions between trapped MgH (MgD) and surrounding H$_2$, D$_2$, or HD. In solid parahydrogen the site absorption of MgH was simplified: only a very sharp band at 1427.4 cm^{-1} and a weak site at 1429.9 cm^{-1} were observed.

In solid neon MgH and MgD give weak bands at 1431.3 and 1045.5 cm^{-1} and the assignment was confirmed by production of the same bands from the Mg atom reaction with HD in solid neon. The absorptions for MgH and MgD in neon are very close to gas-phase fundamentals at 1431.98 and 1045.85 cm^{-1}.[30]

In solid normal hydrogen a weak band at 1464.6 cm^{-1} appeared on deposition, decreased on $\lambda > 320$ nm photolysis, and was partly restored on 193 nm eximer irradiation (recall MgH was also partly restored on 193 nm photolysis). This band was favored by higher laser energy and located 37.5 cm^{-1} higher than the MgH stretching motion. In solid parahydrogen a similar band appeared at 1466.7 cm^{-1}. The deuterium counterpart was found at 1066.7 cm^{-1} for normal D$_2$ and 1068.7 cm^{-1} for ortho-D$_2$. With Mg in solid HD two bands at 1464.3 and 1067.8 cm^{-1} are associated with the bands observed in solid H$_2$ and D$_2$ (the solid molecular hydrogen matrix environments are different). In solid neon the counterpart bands were observed at 1470.0 cm^{-1} in the Mg−H region, 1070.9 cm^{-1} in the Mg−D region, and 1470.0 and 1070.9 cm^{-1} with HD. This is the only feature increased by 193 nm radiation in solid neon. Apparently only one H atom is involved in this vibration motion. The Mg$_2$H molecule is appropriate for this band.

Two isomers of Mg$_2$H, namely MgMgH amd MgHMg, were calculated with the B3LYP functional and MgMgH is energetically favored (Table 3). The predicted Mg−H stretching frequency at 1506.7 cm^{-1} matches our experimental observation very well. However, no band was observed for MgHMg.

The MgH is generated through energetic laser-ablated Mg atom reaction with H$_2$, which is endothermic by 72 kcal/mol for the ground Mg (3s, ^{1}S$_0$) reaction with H$_2$ based on our B3LYP functional calculation or 74 kcal/mol from experiment.[33] However, excited Mg (3s3p, ^{1}P$_1$) is sufficient to overcome this and activate the H−H bond efficiently to give MgH$_2$* and then decompose to MgH and H. Reaction 9 has been studied with pump−probe laser and far-wing laser scattering.[34−36]

$$\text{Mg (3s3p)} + \text{H}_2 \rightarrow \text{MgH}_2^* \rightarrow \text{MgH} + \text{H} \quad (9)$$
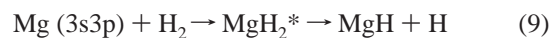
Mg$_2$H is probably formed by clustering with MgH, reaction 10, or by dissociation of HMgMgH, reaction 11.

$$\text{Mg} + \text{MgH} \rightarrow \text{MgMgH} \quad (10)$$

$$\text{HMgMgH} \xrightarrow{193 \text{ nm}} \text{H} + \text{MgMgH} \quad (11)$$

Mg$_2$H$_2$. The sharp, weak absorption at 1486.1 cm^{-1} in solid n-H$_2$ decreased on irradiation like the 1064.8 cm^{-1} Mg$_2$H band. This band shifted to 1083.0 cm^{-1} with n-D$_2$, but unlike Mg$_2$H, different 1495.7 and 1088.9 cm^{-1} counterparts were observed with pure HD.

The counterpart absorption at 1496.4 cm^{-1} for the Mg atom reaction with H$_2$ in solid neon was produced on $\lambda > 240$ nm photolysis but decreased by 193 nm irradiation. With D$_2$ in neon this band shifted to 1088.9 cm^{-1}, but for HD in neon two corresponding bands at 1508.9 and 1099.3 cm^{-1} were observed. These shifts characterize two coupled Mg−H stretching modes, which interact slightly more than in MgH$_2$. Calculations with

Magnesium Hydrides, Complexes, and Dihydrides

J. Phys. Chem. A, Vol. 108, No. 52, 2004 **11519**

TABLE 5: Comparison of Matrix Frequencies (cm⁻¹) for MgH, MgH₂, and Mg₂H₄

molecule	gas[a]	Ne	p-H₂[b]	n-H₂[c]	Ar[d]	Kr[e]	Xe[e]
MgH	1431.98	1431.3	1427.4	1427.1	1422.1		
MgD	1045.85	1045.5	1043.0	1042.8	1037.7		
H/D	1.3692	1.3690	1.3686	1.3685	1.3690		
MgH₂	1588.67	1576.8	1577.4	1569.5	1571.9	1558	1544
MgD₂		1163.2	1163.9	1161.4	1157.1	1153	1144
H/D		1.3556	1.3555	1.3514	1.3546	1.351	1.350
Mg₂H₄		1169.9	1168.2	1170.5	1164.2		
		1058.9	1057.1	1058.7			

[a] References 6 and 30. [b] 99% p-H₂, but for MgD and MgD₂ this is 98% o-D₂. [c] For MgD and MgD₂ this is n-D₂. [d] Reference 7. [e] Reference 8.

the B3LYP functional give a linear HMgMgH geometry with the Mg−H stretching mode at 1551.3 cm⁻¹ and Mg−D at 1119.2 cm⁻¹. In addition HMgMgD stretching modes were predicted at 1561.8 and 1127.0 cm⁻¹, 9.5 cm⁻¹ above the all-H mode and 7.8 cm⁻¹ above the all-D mode (experimental shifts are 12.5 and 9.4 cm⁻¹ in solid neon, and 9.6 and 5.9 cm⁻¹ in solid hydrogen). This means that an unobserved high-symmetry mode is higher in frequency (i.e., the σ_u mode for the linear molecule, Table 3). Such excellent agreement confirms the observation and characterization of linear HMgMgH. The bands assigned formerly[7] to cyclic (MgH)₂ are probably due to H(MgH)₂H or other higher magnesium hydride. Thus, the higher energy cyclic (MgH)₂ species remains unobserved.

Mg₂H₂ is produced from either the Mg₂ reaction with H₂ or the dimerization of MgH. Solid neon experiments gave a clue that Mg₂ is exited by $\lambda > 240$ nm photolysis and combined with H₂ to give Mg₂H₂ (reaction 12) while MgH is not changed. The bonding of Mg₂H₂ is basically the same as that of the magnesium cluster Grignard reagent, where the strong Mg−Mg bond stabilizes this reactive species. In solid hydrogen larger magnesium clusters (HMg$_x$H) are probably formed.

$$Mg_2 + H_2 \xrightarrow{UV} Mg_2H_2 \qquad (12)$$

$$2MgH \rightarrow Mg_2H_2 \qquad (13)$$
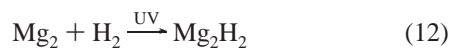
Mg₂H₃. In solid normal hydrogen two bands at 1105.9 and 985.5 cm⁻¹ appeared on deposition, decreased on 380 and 240 nm photolysis, and were restored partly on annealing. The deuterium counterparts were found at 813.1 and 718.5 cm⁻¹ in solid normal D₂. Two modes are just below the double bridged −Mg(μ-H)₂Mg− vibrations in Mg₂H₄ and a similar structure for the new molecule is suggested. Recall two stretching frequencies of double bridged Al(μ-H)₂Al in Al₂H₅ radical are a few wavenumbers below the same modes for dialane,[11] and we believe the Mg₂H₃ radical with a double-bridged Mg(μ-H)₂Mg bond is the case here. First the chemical behavior of this species is very active, and it grows at the expense of both MgH and MgH₂ on early annealing in our experiments. Second B3LYP calculation gave two conformers, single-bridged (HMg-(H)MgH), s-Mg₂H₃, and double-bridged (HMg(μ-H)₂Mg), d-Mg₂H₃, and the latter is 12.1 kcal/mol lower in energy. The stronger and a weaker double-bridged modes of d-Mg₂H₃ were predicated at 1162.2 and 1042.8 cm⁻¹, which match observed values very well after the same adjustment as for Mg₂H₄. Finally, the HD spectra gave additional information for this radical: a stronger band at 1013.9 cm⁻¹ and a weaker band at 814.6 cm⁻¹ in solid HD formed on deposition and disappeared on 240 nm photolysis. Four possible isotopomers with HD, HMg(μ-HD)₂Mg, DMg(μ-HD)₂Mg, HMg(μ-D)₂Mg, and DMg-(μ-H)₂Mg, are computed, and for each of these the strongest absorptions are found at 1105.6, 1103.8, 836.7, and 1162.0 cm⁻¹, respectively. Obviously, the 1013.9 cm⁻¹ band is due to

HMg(μ-HD)₂Mg and DMg(μ-HD)₂Mg and the 814.6 cm⁻¹ band is due to HMg(μ-D)₂Mg based on calculated frequencies with scaled corrections. Again the preference is for the heavier isotope in the bridge position. The combination of MgH₂ and MgH is exothermic by 25.6 kcal/mol (B3LYP).

$$MgH + MgH_2 \rightarrow d\text{-}Mg_2H_3 \qquad (14)$$

Matrix Shifts. The large number of new magnesium hydride species provides further subjects for unusual matrix shifts. First, MgH behaves quite normally in that the fundamental frequency decreases from left to right in Table 5. Note that the MgH frequency in p-H₂ is red-shifted 4.6 cm⁻¹ from the gas phase whereas the frequency is red-shifted 4.9 cm⁻¹ in n-H₂. Analogous results are found for MgD in o-D₂ and n-D₂. The H/D frequency ratios are 1.3692−1.3690 for gas, Ne, and Ar frequencies, but slightly lower 1.3686 and 1.3685 values are observed in the solid hydrogens. This is consistent with slightly less H motion in the Mg−H vibration due to greater interaction with the hydride and the hydrogen matrix cage.

The MgH₂ frequencies reveal a small difference from the trend found for MgH in different matrices: The p-H₂ frequency for MgH₂ is 0.6 cm⁻¹ higher than the neon value, and the o-D₂ frequency for MgD₂ is 0.7 cm⁻¹ higher than the neon value. The n-H₂ and n-D₂ frequencies are lower than the neon values and the gas-phase values,[6] as expected. The p-H₂ environment perturbs the linear MgH₂ molecule less than neon even though very weak complexes are formed with H₂. The H/D ratios again provide evidence for less H motion in n-H₂, Kr, and Xe due to stronger interaction with the hydride. Figure 4 compares the spectra in normal and $J = 0$ enriched molecular hydrogens.

Note that the matrix shifts for MgH₂ are larger than those for MgH even with p-H₂. This is due to stronger H₂ complex formation with MgH₂ than with MgH: even though bond polarity is the same (B3LYP Mulliken charges are −0.19 on H in both MgH and MgH₂), the Mg charge is +0.38 in MgH₂ as compared to +0.19 in MgH.

Finally, HMg(μ-H)₂MgH is unusual in that the n-H₂ frequencies are highest. However, these are Mg−H−Mg bridge bond stretching modes, and a stronger interaction may help relieve electron deficiency and strengthen the bridge bonds. The same relationship was found for dialane, H₂Al(μ-H)₂AlH₂. The terminal Al−H modes are slightly higher in p-H₂, but the bridge Al−H−Al modes are slightly lower in p-H₂ as compared to n-H₂.[11]

Conclusions

Laser ablated Mg atoms react with H₂ in excess neon and hydrogen on co-deposition to give MgH and MgH₂. The absorption of MgH at 1431.3 cm⁻¹ in solid neon is essentially the same as detected in the gas phase at 1431.98 cm⁻¹. In solid parahydrogen MgH shifts to 1427.4 cm⁻¹ showing weak interaction with surrounding H₂. The Mg−H stretching mode

of MgH_2 at 1576.2 cm^{-1} in solid neon is 12.5 cm^{-1} lower than the recent gas-phase value,[6] indicating that the HMgH molecule interacts with surrounding neon atoms stronger than MgH. In fact stronger interaction was found for HMgH with H_2 in solid H_2 based on two strong H−H stretching modes induced by MgH_2. We suggest H_2 molecules are associated side-on to Mg and end-on to H surrounding HMgH, and theoretical calculations support this model.

Dimagnesium hydrides, Mg_2H, Mg_2H_2, Mg_2H_3, and Mg_2H_4, were identified using isotopic substitutions and theoretical calculations. A strong Mg−Mg bond is favored in hydrogen-deficient molecules such as Mg_2H and Mg_2H_2, while double bridged Mg−H−Mg bonds were found in Mg_2H_3 and Mg_2H_4. The latter molecule $HMg(\mu$-H$)_2MgH$ is analogous to dialane[9−11] $H_2Al(\mu$-H$)_2AlH_2$, but both terminal and bridged bonds are computed to be 7.8% longer in the magnesium compound.

References and Notes

(1) (a) Schlapbach, L.; Zuttel, A. *Nature* **2001**, *414*, 353. (b) Dresselhaus, M. S.; Thomas, I. L. *Nature* **2001**, *414*, 332.

(2) Aldridge, S.; Downs, A. J. *Chem. Rev.* **2001**, *101*, 3305.

(3) Grochala, W.; Edwards, P. P. *Chem. Rev.* **2004**, *104*, 1283.

(4) Zachariasen, W. H.; Holley, C. E.; Stampfer, J. F. *Acta Crystallogr.* **1963**, *16*, 352.

(5) Santisteban, J. R.; Cuello, G. J.; Dawidowski, J.; Fainstein, A.; Peretti, H. A.; Ivanov, A.; Bermejo, F. J. *Phys. Rev. B* **2000**, *62*, 37.

(6) (a) Shayesteh, A.; Appadoo, D. R. T.; Gordon, I.; Bernath, P. F. *J. Chem. Phys.* **2003**, *119*, 7785. (b) Shayesteh, A.; Appadoo, D. R. T.; Gordon, I.; Bernath, P. F. *Can. J. Phys.* **2004**, *82*, 947.

(7) Tague, T. J., Jr.; Andrews, L. *J. Phys. Chem.* **1994**, *98*, 8611.

(8) McCaffrey, J. G.; Parnis, J. M.; Ozin, G. A.; Breckenridge, W. H. *J. Phys. Chem.* **1985**, *89*, 4945.

(9) Andrews, L.; Wang, X. *Science* **2003**, *299*, 2049.

(10) Wang, X.; Andrews, L.; Tam, S.; DeRose, M. E.; Fajardo, M. J. *Am. Chem. Soc.* **2003**, *125*, 9218.

(11) Andrews, L.; Wang, X. *J. Phys. Chem. A* **2004**, *108*, 4202 (Al + H_2).

(12) Wang, X.; Andrews, L. *J. Phys. Chem. A* **2003**, *107*, 11371 (Ga + H_2).

(13) Andrews, L.; Wang, X. *Angew. Chem., Int. Ed.* **2004**, *43*, 1706.

(14) Wang, X.; Andrews, L. *J. Phys. Chem. A* **2004**, *108*, 4440 (In + H_2).

(15) Wang, X.; Andrews, L. *J. Phys. Chem. A* **2004**, *108*, 3396 (Tl + H_2).

(16) Andrews, L.; Citra, A. *Chem. Rev.* **2002**, *102*, 885 and references therein.

(17) Andrews, L. *Chem. Soc. Rev.* **2004**, *33*, 123 and references therein.

(18) Wang, X.; Andrews, L. *J. Phys. Chem. A* **2004**, *108*, 1103 ((H_2)$_n$(H$^-$)).

(19) Andrews, L.; Wang, X. *Rev. Sci. Instrum.* **2004**, *75*, 3039.

(20) Wang, X.; Wolfe, B.; Andrews, L. *J. Phys. Chem. A* **2004**, *108*, 5169.

(21) Frisch, M. J.; Trucks, G. W.; Schlegel, H. B.; Scuseria, G. E.; Robb, M. A.; Cheeseman, J. R.; Zakrzewski, V. G.; Montgomery, J. A., Jr.; Stratmann, R. E.; Burant, J. C.; Dapprich, S.; Millam, J. M.; Daniels, A. D.; Kudin, K. N.; Strain, M. C.; Farkas, O.; Tomasi, J.; Barone, V.; Cossi, M.; Cammi, R.; Mennucci, B.; Pomelli, C.; Adamo, C.; Clifford, S.; Ochterski, J.; Petersson, G. A.; Ayala, P. Y.; Cui, Q.; Morokuma, K.; Malick, D. K.; Rabuck, A. D.; Raghavachari, K.; Foresman, J. B.; Cioslowski, J.; Ortiz, J. V.; Stefanov, B. B.; Liu, G.; Liashenko, A.; Piskorz, P.; Komaromi, I.; Gomperts, R.; Martin, R. L.; Fox, D. J.; Keith, T.; Al-Laham, M. A.; Peng, C. Y.; Nanayakkara, A.; Gonzalez, C.; Challacombe, M.; Gill, P. M. W.; Johnson, B.; Chen, W.; Wong, M. W.; Andres, J. L.; Gonzalez, C.; Head-Gordon, M.; Replogle, E. S.; Pople, J. A. *Gaussian 98*, Revision A.11.4, Gaussian, Inc.: Pittsburgh, PA, 1998, and references therein.

(22) Gush, H. P.; Hare, W. F.; Allin, E. J.; Welsh, H. L. *Can. J. Phys.* **1960**, *38*, 176.

(23) Crane, A.; Gush, H. P. *Can. J. Phys.* **1966**, *44*, 373.

(24) Andrews, L.; Wang, X. *J. Phys. Chem. A* **2004**, *108*, 3879.

(25) Momose, T.; Shida, T. *Bull. Chem. Soc. Jpn.* **1998**, *71*, 1.

(26) Pople, J. A.; Luke, B. T.; Frisch, M. J.; Binkley, J. S. *J. Phys. Chem.* **1985**, *89*, 2198.

(27) Tschumper, G. S.; Schaefer, H. F., III *J. Chem. Phys.* **1998**, *108*, 7511.

(28) Von Szentpaly, L. *J. Phys. Chem. A* **2002**, *106*, 11945.

(29) Kaupp, M.; Schleyer, P. v. R. *J. Am. Chem. Soc.* **1993**, *115*, 11202.

(30) Lemoine, B.; Demuynck, C.; Destombes, J. L.; Davies, P. B. *J. Chem. Phys.* **1988**, *89*, 673.

(31) Miller, J. C.; Andrews, L. *J. Am. Chem. Soc.* **1978**, *100*, 2966.

(32) Stander, C. M.; Pacey, R. A. *J. Phys. Chem. Solids* **1978**, *39*, 829.

(33) Huber, K. P.; Herzberg, G. *Spectra of Diatomic Molecules*; Van Nostrand Reinhold: New York, 1979.

(34) (a) Kleiber, P. D.; Lyyra, A. M.; Sando, K. M.; Heneghan, S. P.; Stwalley, W. C. *Phys. Rev. Lett.* **1985**, *54*, 2003. (b) Kleiber, P. D.; Lyyra, A. M.; Sando, K. M.; Zafiropulos, V.; Stwalley, W. C. *J. Chem. Phys.* **1986**, *85*, 5493.

(35) (a) Breckenridge, W. H.; Wang, J. H. *Chem. Phys. Lett.* **1987**, *137*, 195. (b) Breckenridge, W. H. *J. Phys. Chem.* **1996**, *100*, 14840.

(36) Liu, D. K.; Lin, K. C. *Chem. Phys. Lett.* **1997**, *274*, 37.